This issue replaces and supersedes all previous issues of this report.

29

SID 62-1437-R-1

STATIC STABILITY AND FORCE CHARACTERISTICS OF A 0.02-SCALE MODEL OF THE SATURN C-1 LAUNCH VEHICLE WITH APOLLO PAYLOAD FOR THE MACH NUMBER RANGE 3.5 TO 8.0 NAS9-150 (U)

Reissued April 1963

NORTH AMERICAN AVIATION, INC.
SPACE and INFORMATION SYSTEMS DIVISION

CONFIDENTIAL

FOREWORD

The tests to determine static stability and force characteristics of the launch vehicle model were conducted under NASA Contract NAS9-150.

This report was prepared by G. E. Frantz of the Columbus Division of North American Aviation, Inc.

CONFIDENTIAL

SUMMARY

The static stability and force characteristics of the launch, launch-abort, and second-stage configurations of a 0.02-scale model of the Saturn C-1 launch vehicle with Apollo payload were investigated in the Arnold Center VKF Wind Tunnels A and B at the Mach number range 3.5 to 8.0.

The escape system induced separated flow over the forebody and thereby produced a significant effect on the force characteristics of both the launch and the second-stage configurations. The second-stage aerodynamic characteristics were also influenced by small Reynolds number variations and by the presence of the launch escape system flow separator. Neither Reynolds number nor the flow separator had significant effects on the launch configuration characteristics.

The aerodynamic coefficients for all configurations tested were essentially insensitive to roll attitude.

CONFIDENTIAL

CONTENTS

CONFIDENTIAL

ILLUSTRATIONS

I. INTRODUCTION

Static stability and force characteristics of the Saturn C-1 launch vehicle with Apollo payload are being investigated with a 0.02-scale model (FSL-1) in the Mach number range from 0.3 to 8.0. This program consists of a series of wind tunnel tests at four facilities: Ames Research Center, Arnold Engineering Development Center, North American Aviation TWT, and North American Aviation NACAL. This report presents the analysis of the results of the tests conducted in the Arnold Center von Karman Facility Wind Tunnels A and B from 1 October to 9 October 1962. The basic data from the AEDC tests are presented in the data report.[1]

The AEDC tests were conducted to determine the static stability and force characteristics of (1) the launch and launch-abort configurations at or near flight Reynolds numbers in the Mach number range from 3.5 to 8.0 and (2) the second-stage configurations at flight Reynolds numbers for a Mach number of 8.0. The effects of Reynolds number variations and launch escape system flow separator were also investigated.

---

[1] Data Report for the Apollo Model (FSL-1) Wind Tunnel Tests in the A and B Tunnels of the AEDC von Karman Gas Dynamics Facility. NAA/S&ID SID 62-1144.

II. MODEL AND TESTS

MODEL

The 0.02-scale model consisted of the complete launch configuration (FSL-1) of the Apollo payload with the Saturn C-1 launch vehicle. By removing sections of the model, five basic configurations were obtainable: launch ($B_3I_2S_4R_4C_2T_{20}E_{40}$), launch-abort ($B_3I_2S_4R_4$), second stage with escape system ($B_4I_2S_4R_4C_2T_{20}E_{40}$), second stage ($B_4I_2S_4R_4C_2$), and second stage with service module and command module removed ($B_4I_2S_5$). The launch escape system flow separator and jet reaction controls were also removable. Detailed descriptions and drawings of the model and typical model installations are contained in the test and model information report.[1] Sketches of the configurations tested are presented in Figure 1; photographs of the configurations are shown in Figures 2 through 6.

TESTS

The launch and launch-abort configurations were tested at Mach numbers of 3.5, 4.0, 4.5, 5.0, and 6.0 in the von Karman Facility (VKF) A tunnel and at a Mach number of 8.0 in the VKF B tunnel. The second-stage configurations were tested at a Mach number of 8.0 in the VKF B tunnel.

The launch and launch-abort configurations were installed on the VKF 3302475 balance assembly and were mounted on the LH 101-9 sting in tunnel A and on the VKF 3302122 sting in tunnel B. The VKF 33022180 balance assembly and VKF 3302122 sting were used for testing the second-stage configurations. The balances measured axial, normal, and side forces as well as pitching, yawing, and rolling moments. One static pressure measured in the balance chamber was assumed to represent the actual base pressure acting on the model base.

The effects of Reynolds number variations and the launch escape system flow separator were investigated at Mach numbers 6.0 and 8.0.

Data were obtained for angles of attack from -4 to 15 degrees at sideslip angles of -6, -3, 0, and 3 degrees. Sideslip was obtained by rolling the model while at an angle of attack.

---

[1] Test and Model Information for Wind Tunnel Tests of a 0.02-Scale Force Model (FSL-1) of the Apollo in the Arnold Center VKF Wind Tunnels A, B, and C. NAA/S&ID SID 62-806.

CONFIDENTIAL

A complete list of the specific tests conducted is presented in Table 1.

Transition grit was not used since the tests were conducted at or near flight Reynolds numbers. The variation of tunnel Reynolds number with Mach number is presented in Figure 7. The points connected by a solid line in this illustration represent basic test Reynolds numbers.

Table 1. Index of Completed Runs at AEDC

Configuration	P_T (psia)	T_o (^oF)	Mach Number																	
			3.5				4.0				4.5				5.0				6.0				8.0			
			β																					
			-6	-3	0	+3	-6	-3	0	+3	-6	-3	0	+3	-6	-3	0	+3	-6	-3	0	+3	-6	-3	0	+3
			Group Number																							
$B_3I_2S_4R_4C_2T_{20}E_{40}$	35	210																			41					
	57	111	4	3	1	2																				
	75	111					8	7	5	6																
	85	220																	40	39	37	38				
	116	108									12	11	9	10												
	140	195													16	15	13	14								
	175	865																					9	8	6	7
$B_3I_2S_4R_4C_2T_{20}E_{35}$	85	210																			42					
	175	865																							10	
$B_3I_2S_4R_4$	57	111	20	19	17	18																				
	75	111					24	23	21	22																
	85	220																	36	35	33	34				
	116	108									28	27	25	26												
	140	195													32	31	29	30								
	175	865																					4	3	1	2
	175	865																							5	
$B_4I_2S_4R_4C_2T_{20}E_{40}$	175	865																					14	13	11	12
	600	875																							15	
$B_4I_2S_4R_4C_2T_{20}E_{35}$	175	865																							16	
$B_4I_2S_5$	175	865																					20	19	17	18
$B_4I_2S_4R_4C_2$	175	865																					24	23	21	22

Note: Runs at Mach 3.5 to 6.0 were made in Tunnel A. Runs at Mach 8.0 were accomplished in Tunnel B. The two independent tests account for redundancy in assigning group (run) numbers.

CONFIDENTIAL

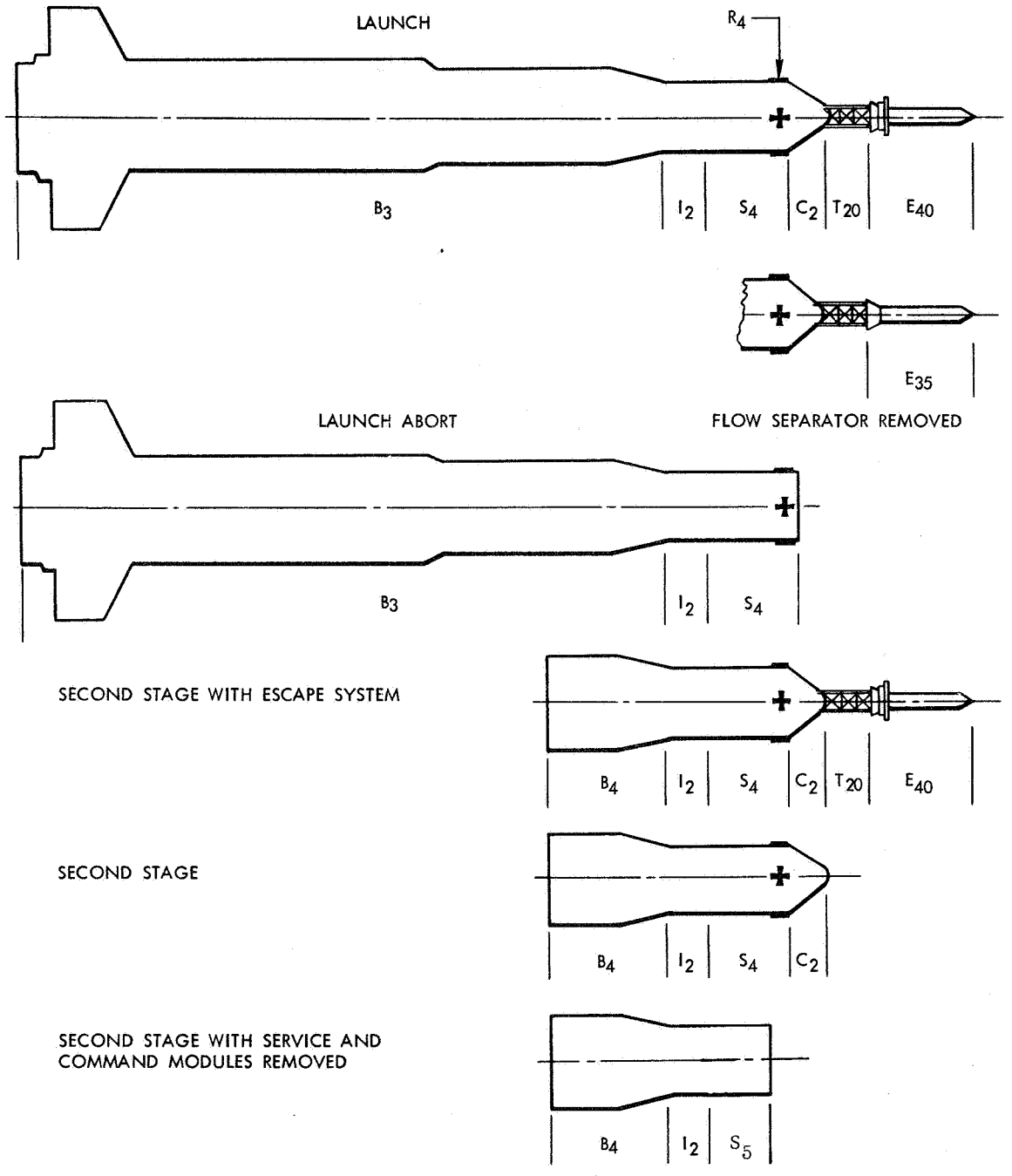

Figure 1. Test Configuration

CONFIDENTIAL

CONFIDENTIAL

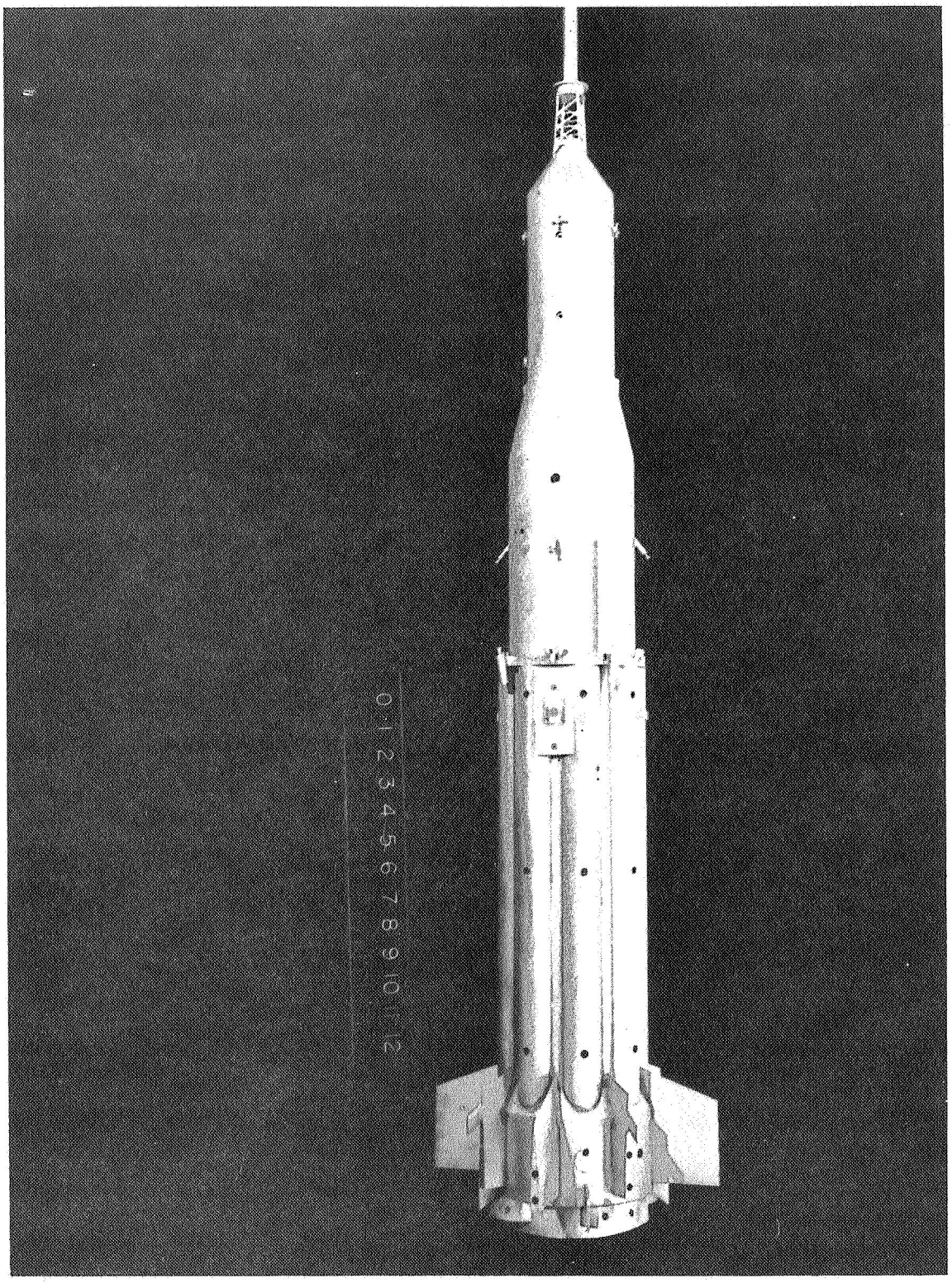

Figure 2. Launch Configuration

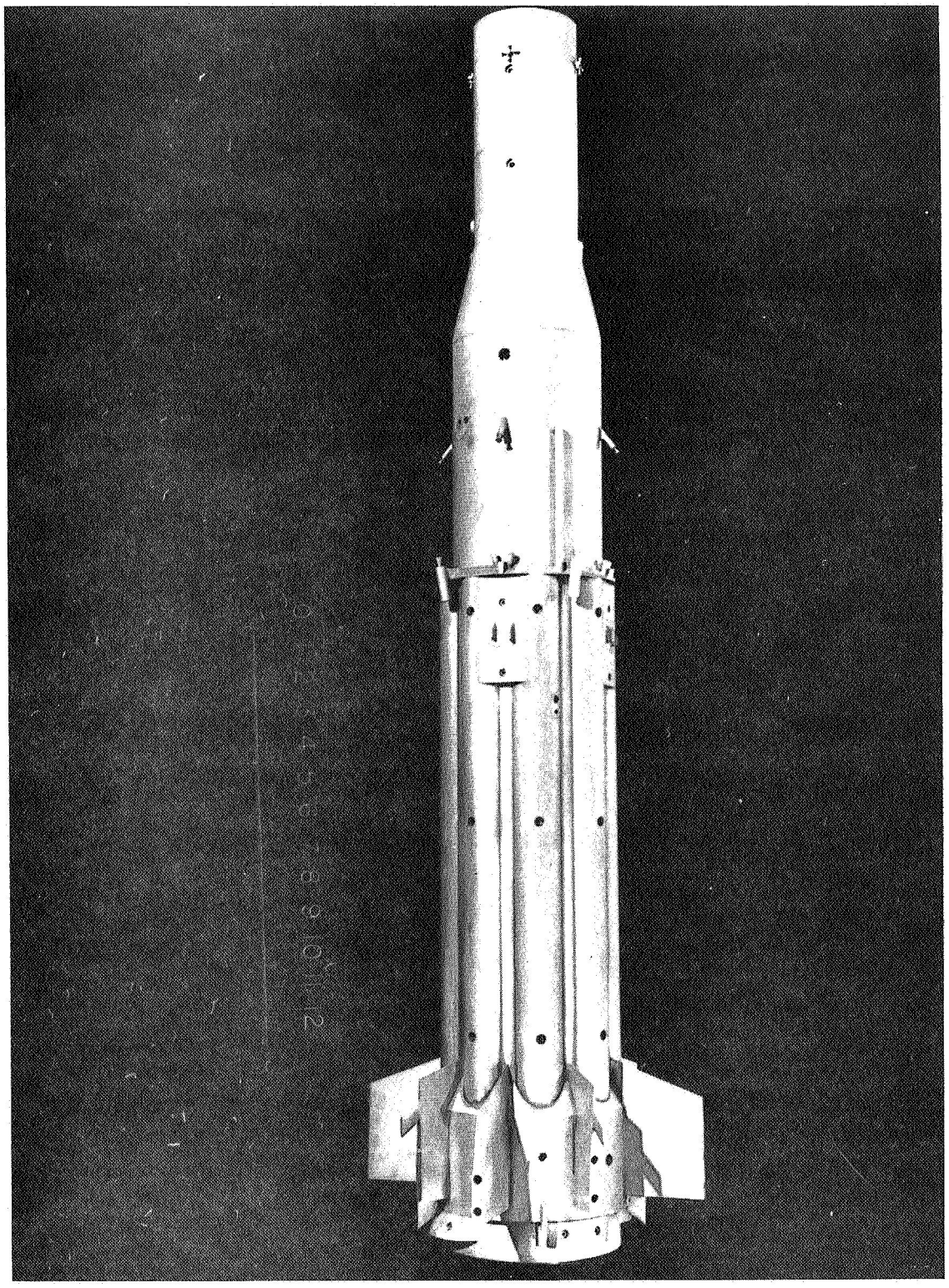

Figure 3. Launch-Abort Configuration

CONFIDENTIAL

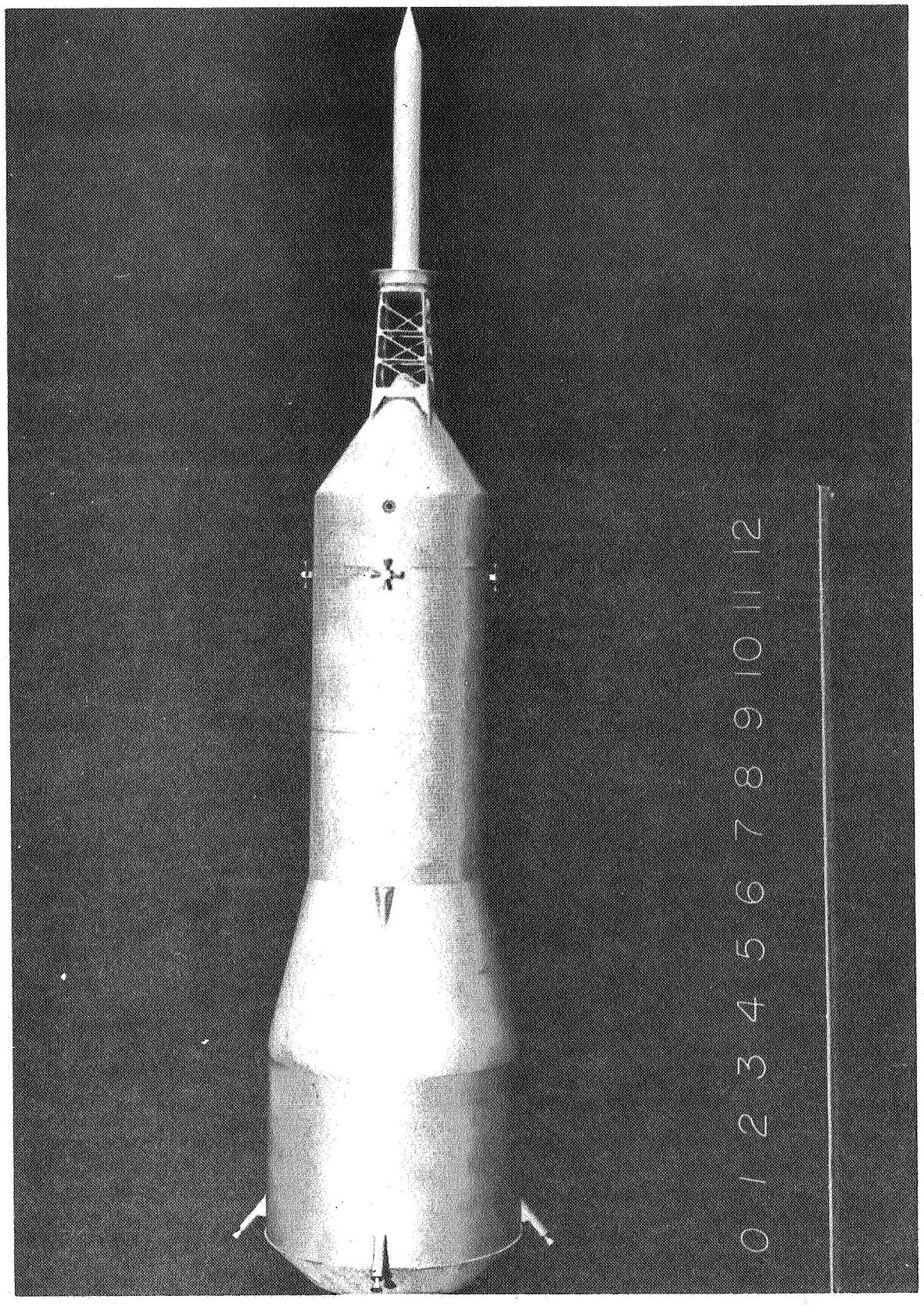

Figure 4. Second-Stage Configuration With Escape System

CONFIDENTIAL

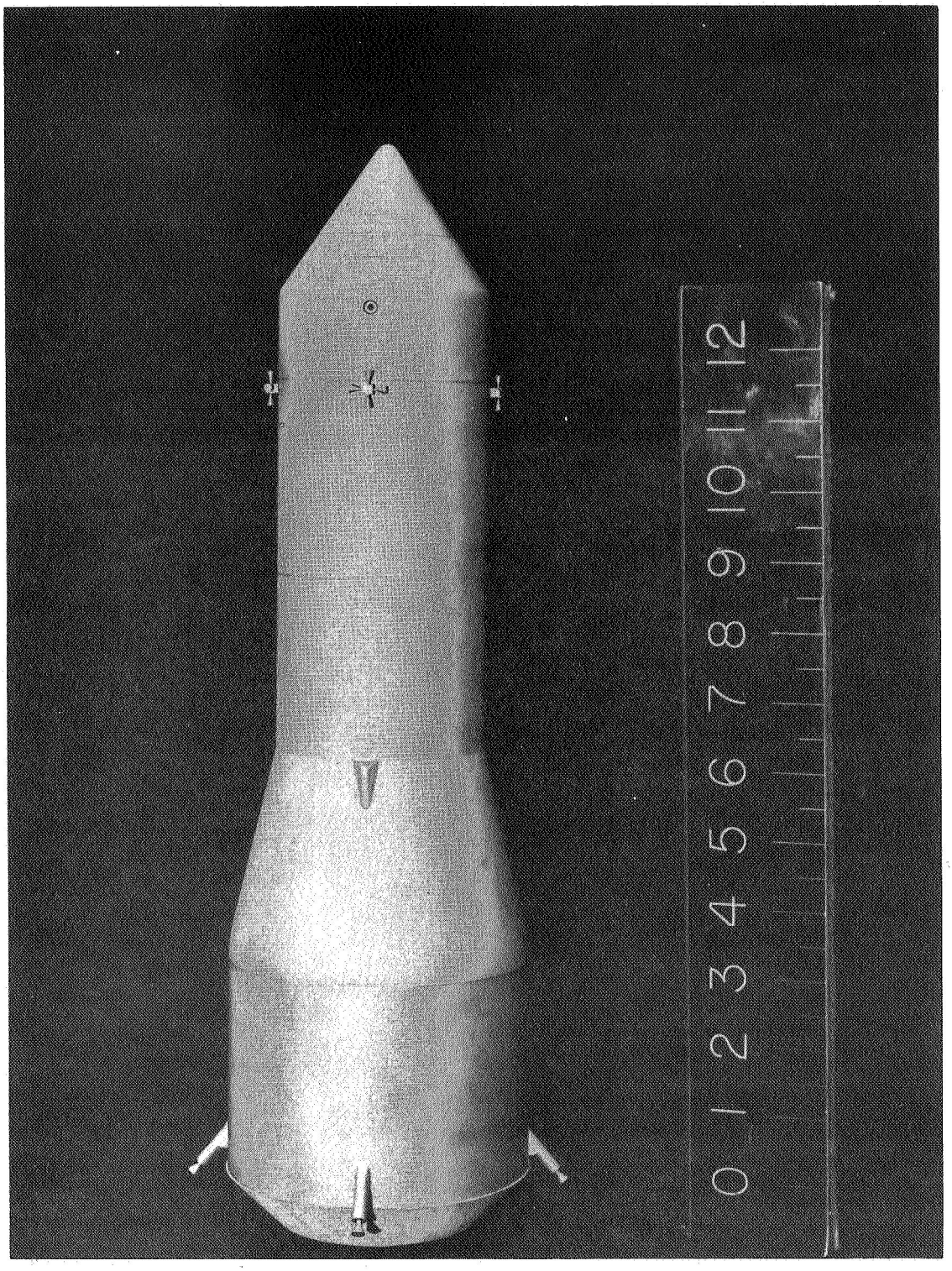

Figure 5. Second-Stage Configuration

CONFIDENTIAL

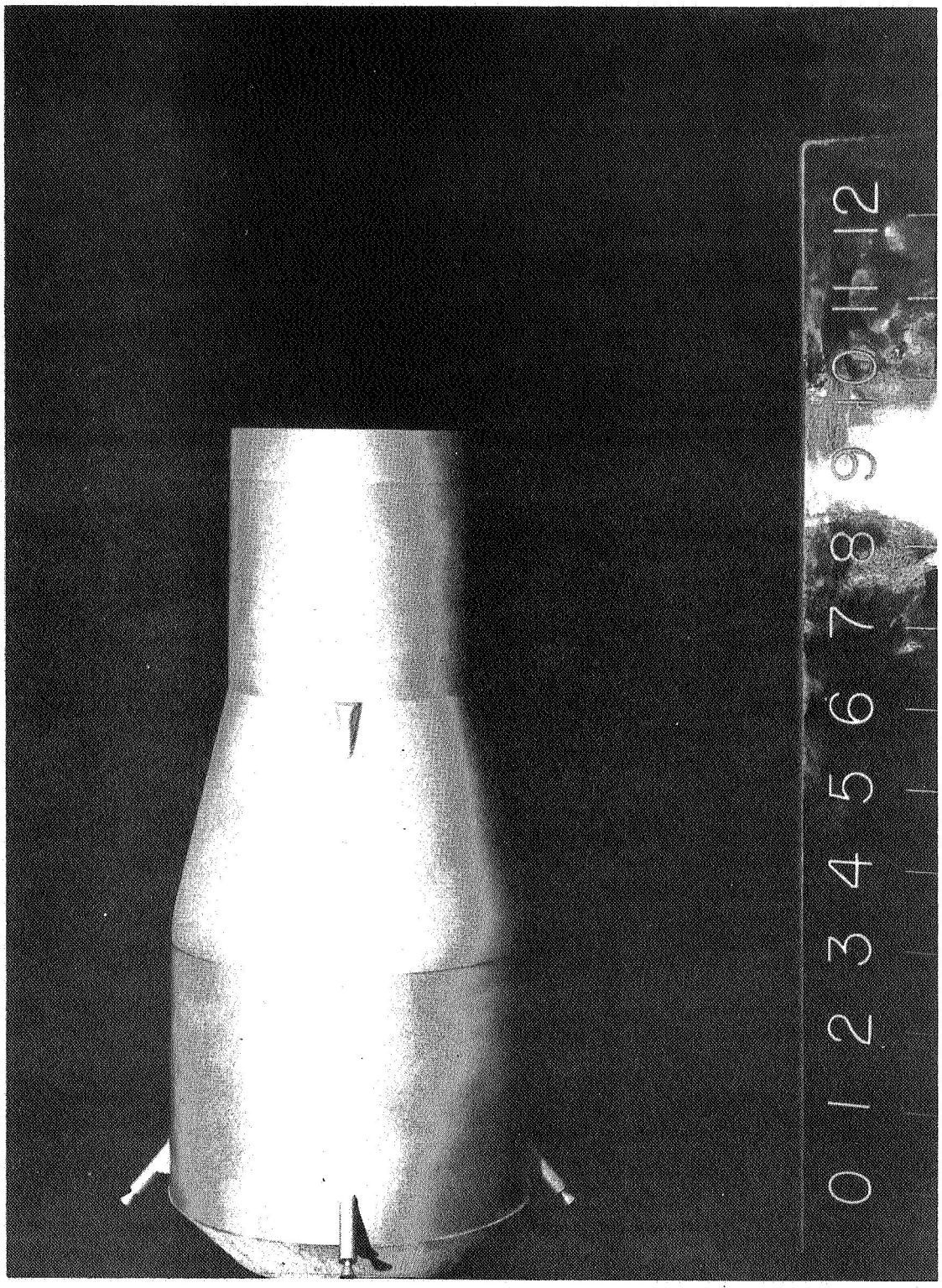

Figure 6. Second-Stage Configuration With Service Module and Command Module Removed

CONFIDENTIAL

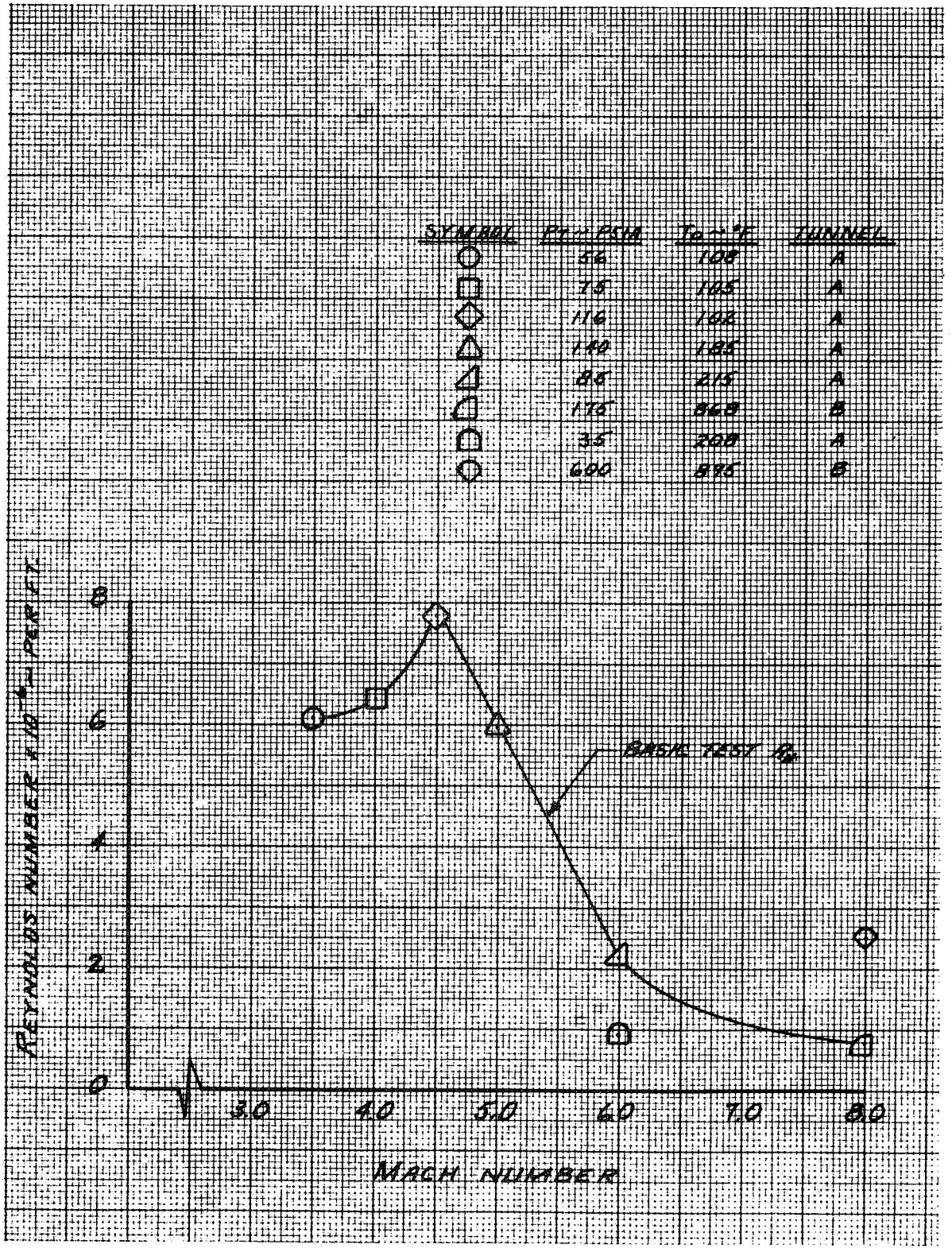

Figure 7. Variation of Tunnel Reynolds Number With Mach Number

CONFIDENTIAL

III. RESULTS AND DISCUSSION

PRESENTATION OF RESULTS

Summary results of the test data are presented in the form of C_{N_α}, C_{m_α}, X_{cp}/D, C_A, and C_{P_b} versus Mach number for the launch and launch-abort configurations. All coefficients presented herein for the launch and launch-abort configurations are based on booster frontal area (0.1440 ft^2) and diameter (0.4283 ft), and referenced to a moment center, which represents the gimbal station, located 0.389 booster diameters forward of the base (model station 0.00). Note that these reference dimensions are different from those used in the Ames tests.[1] Summary results of the test data for the second-stage configurations, which were tested at Mach number 8.0 only, are presented in tabular form. The coefficients presented for the second-stage configurations are based on command module frontal area (0.0517 ft^2) and diameter (0.2567 ft) and are referenced to a moment center based on a representative center of mass located 8.268 command module diameters forward of the first-stage base. The reference dimensions used for this report are summarized below. Subscripts 1 and 2 are used to differentiate between the two groups of reference dimensions.

Launch and Launch-Abort Configurations

A_{b_1}	Model base area	0.1364 ft^2
D_1	Reference length (booster frontal diameter)	0.4283 ft
S_1	Reference area (booster frontal area)	0.1440 ft^2
$\bar{X}_1$	Location of the reference moment center measured from the model base	0.389 D_1

Second-Stage Configuration

A_{b_2}	Model base area	0.1056 ft^2
D_2	Reference length (command module frontal diameter)	0.2567 ft

[1] Static Stability and Force Characteristics of a 0.02-Scale Model of the Saturn C-1 Launch Vehicle with Apollo Payload for the Mach Number Range 0.70 to 3.50. NAA/S&ID SID 62-1391.

S_2	Reference area (command module frontal area)	0.0517 ft^2
$\overline{X}_2$	Location of the reference moment center measured from the first-stage model base	8.268 D_2

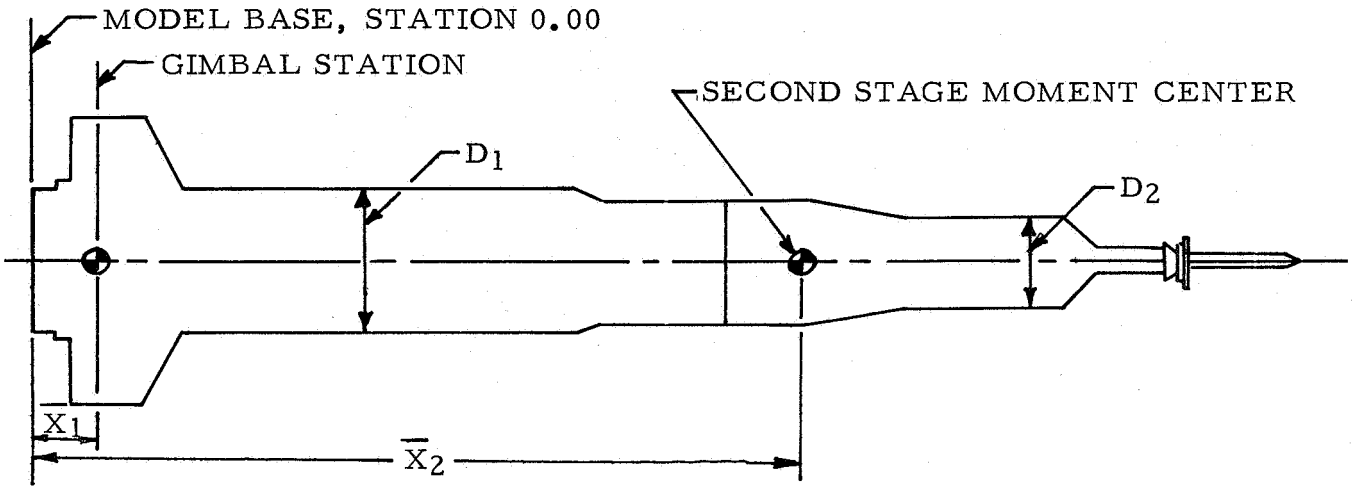

Launch Configuration

Summary curves for the launch configuration are presented in Figure 8. C_{N_α} decreases linearly in the Mach number range 3.5 to 5.0, begins increasing at Mach number 6.0, and increases markedly at Mach number 8.0. C_{m_α} is unstable (for the representative moment center) and remains essentially constant in the Mach number range of 3.5 to 5.0 then exhibits an abrupt increase (more unstable) at Mach number 6.0. The corresponding center of pressure moves forward gradually as the Mach number increases from 3.5 to 5.0, then abruptly shifts forward at Mach number 6.0. The increase in C_{N_α} and C_{m_α} and forward shift of the center of pressure at Mach number 6.0 may be attributed to increased flow separation over the escape rocket, tower, and command module. Increased flow separation not only causes the normal force to increase but also shifts the center of pressure toward the separated region. It is a normal characterisitic of high-speed flow over bodies for flow separation to increase with simultaneously increasing Mach number and decreasing Reynolds number. It is noted that the tests Reynolds number (Figure 7) decreased by a factor of 3 when the Mach number was increased from 5.0 to 6.0.

Comparison of C_{N_α}, C_{m_α}, and X_{cp}/D with the Ames data results for the launch configuration at Mach number 3.5 shows good agreement. A comparison with data obtained in the Chance Vought Aeronautics (CVA) 4- by 4-foot wind tunnel for a similar configuration shows some disagreement. The CVA data indicate a slightly smaller C_{N_α} and a more aft center of pressure. The model tested at CVA did not incorporate the launch escape system flow separator and had a shortened I_2S_4 section. The shortened forebody section would account for the differences in the data.

The axial force coefficients exhibit a typical gradual decrease with Mach number from Mach number 3.5 to 5.0 but a more abrupt decrease at Mach number 6.0. This variation is also a result of increased flow separation at Mach number 6.0. Comparison of the axial force and base pressure coefficients with the Ames data at Mach number 3.5 shows excellent agreement.

Launch-Abort Configuration

Summary data for the launch-abort configuration are presented in Figure 9. From Mach number 3.5 to 6.0, C_{N_α} has the same variation with Mach number (but reduced by a factor of 0.5) as that obtained for the launch configuration. C_{N_α} continues decreasing to a value 32 percent of that obtained for the launch configuration at Mach number 8.0. C_{m_α} is essentially constant with Mach number and indicates a more stable configuration than the launch configuration. The corresponding center of pressure is farther aft by a distance of 1.0 diameter at Mach numbers 3.5 to 5.0 and approximately 2.0 diameters at Mach numbers 6.0 and 8.0. The base pressure coefficient is the same as that obtained for the launch configuration. The axial force coefficient decreases gradually from Mach number 3.5 to 6.0 then increases slightly at Mach number 6.0 and remains constant to Mach number 8.0. The slight increase at Mach number 6.0 is probably caused by increased skin friction drag due to the reduced Reynolds number. The launch-abort data are in good agreement with the Ames data at Mach number 3.5.

Second-Stage Configurations $B4I_2S_4R4C_2T_{20}E_{40}$, $B4I_2S_4R4C_2$, and $B4I_2S_5$

Summary data for the second-stage configurations at Mach number 8.0 are presented in the following tabulation. It should be re-emphasized that the coefficients presented for the second-stage configurations are based on command module area and diameter and are referenced to a moment center located 8.268 command module diameters forward of the first-stage base.

CONFIDENTIAL

Configuration	$(C_{N_\alpha})_{\alpha = 0}$	$(C_{m_\alpha})_{\alpha = 0}$	$(X_{cp}/D)_{\alpha = 0}$	$(C_A)_{\alpha = 0}$
$B_4I_2S_4R_4C_2T_{20}E_{40}$	0.190	0.420	10.478	0.280
$B_4I_2S_4R_4C_2$	0.072	0.135	10.143	0.780
$B_4I_2S_5$	0.028	0.025	9.162	1.970

All three second-stage configurations are unstable about the reference moment center. It is observed that the escape system has a large effect on the aerodynamic characteristics in that the addition of the escape rocket and tower (separator on) roughly triples the C_{N_α} and C_{m_α} and decreases the axial force at $\alpha = 0$ to a value one-third as large. Flow separation over the forebody causes the slope changes and, in part, causes the reduction in axial force coefficient. The axial force is also decreased as a result of the weaker bow compression shock arising from the escape rocket, whereas a much stronger shock exists with the escape system removed.

EFFECT OF REYNOLDS NUMBER VARIATION

A limited investigation was conducted to determine the effect of Reynolds number on the force and moment data. Specifically, the tests conducted were as follows:

Configuration	Mach Number	Reynolds Number per Ft x 10^{-6}
$B_3I_2S_4R_4C_2T_{20}E_{40}$	6.0	2.16 and 0.91
$B_4I_2S_4R_4C_2T_{20}E_{40}$	8.0	0.78 and 2.52

No significant variation or trends attributable to Reynolds number were observed for the launch configuration. However, as shown in Figure 10, a change in Reynolds number resulted in a small change in axial force coefficient for the second-stage configuration with the escape system. The decreased axial force near $\alpha = 0$ for the lower Reynolds number is a result of increased flow separation. The increased C_A above $\alpha = 4$ degrees for the lower Reynolds number is probably caused by increased skin friction drag. No significant effect of Reynolds number on normal force or pitching moment was observed for the second-stage configuration.

CONFIDENTIAL

EFFECT OF FLOW SEPARATOR

To evaluate the effect of the separator, tests were conducted with the separator removed from the launch configuration at Mach numbers 6.0 and 8.0 and from the second-stage configuration at Mach number 8.0. The separator had no significant effect on the launch configuration; however, an effect on the second-stage configuration was observed, and the results are presented in Figure 11 in the form of incremental normal force, axial force, and pitching moment due to the separator. The effect is extremely nonlinear with angle of attack; however, a general decrease in normal force and pitching moment and an increase in axial force may be observed.

EFFECT OF ROLL ATTITUDE

Roll attitude was obtained by rolling the model and sting while conducting pitch runs. The roll angles corresponded to sideslip angles of -6, -3, and 3 degrees and were computed by the equation

$$\text{Tan } \phi = \text{Tan } \beta / \sin \alpha$$

A comparison of $C_{Y\beta}$ at $\alpha = 0$ with $C_{N\alpha}$ at $\beta = 0$ showed no difference. The data were also analyzed on the basis of composite normal force ($\bar{C}_N$) and pitching moment ($\bar{C}_m$) versus composite angle of attack ($\bar{\alpha}$). Comparison of the composite coefficients with the coefficients at $\beta = 0$ showed small differences (less than 10 percent); however, the data scatter was such that no definite trends or variations could be established.

NONLINEARITY OF AERODYNAMIC COEFFICIENTS

The effects of Mach number on C_N, C_m, and C_A for the launch and launch-abort configurations are presented in Figures 12 and 13. At Mach numbers below 6.0, both C_N and C_m for the launch configuration are generally linear with angle of attack up to $\alpha = 6$ degrees. Above Mach number 6.0 where separation effects are noticed, however, C_N and C_m (particularly C_m) become nonlinear at $\alpha = 2$ degrees. The axial force for the launch configuration is minimum at $\alpha = 0$ degrees and becomes less dependent on Mach number as the angle of attack is increased. C_A for the launch-abort configuration is nearly constant with Mach number except at Mach number 5.0 where a slight decrease is observed.

The effect of angle of attack on the aerodynamic coefficients for the second-stage configurations at Mach number 8.0 is presented in Figure 14. To illustrate the influence of the escape system more clearly, incremental effects are shown in Figure 15. It is observed that the effect of the escape system is decreased as angle of attack is increased beyond 4 degrees. This may be explained by noting that interference from the escape system wake decreases with increasing angle of attack.

CONFIDENTIAL

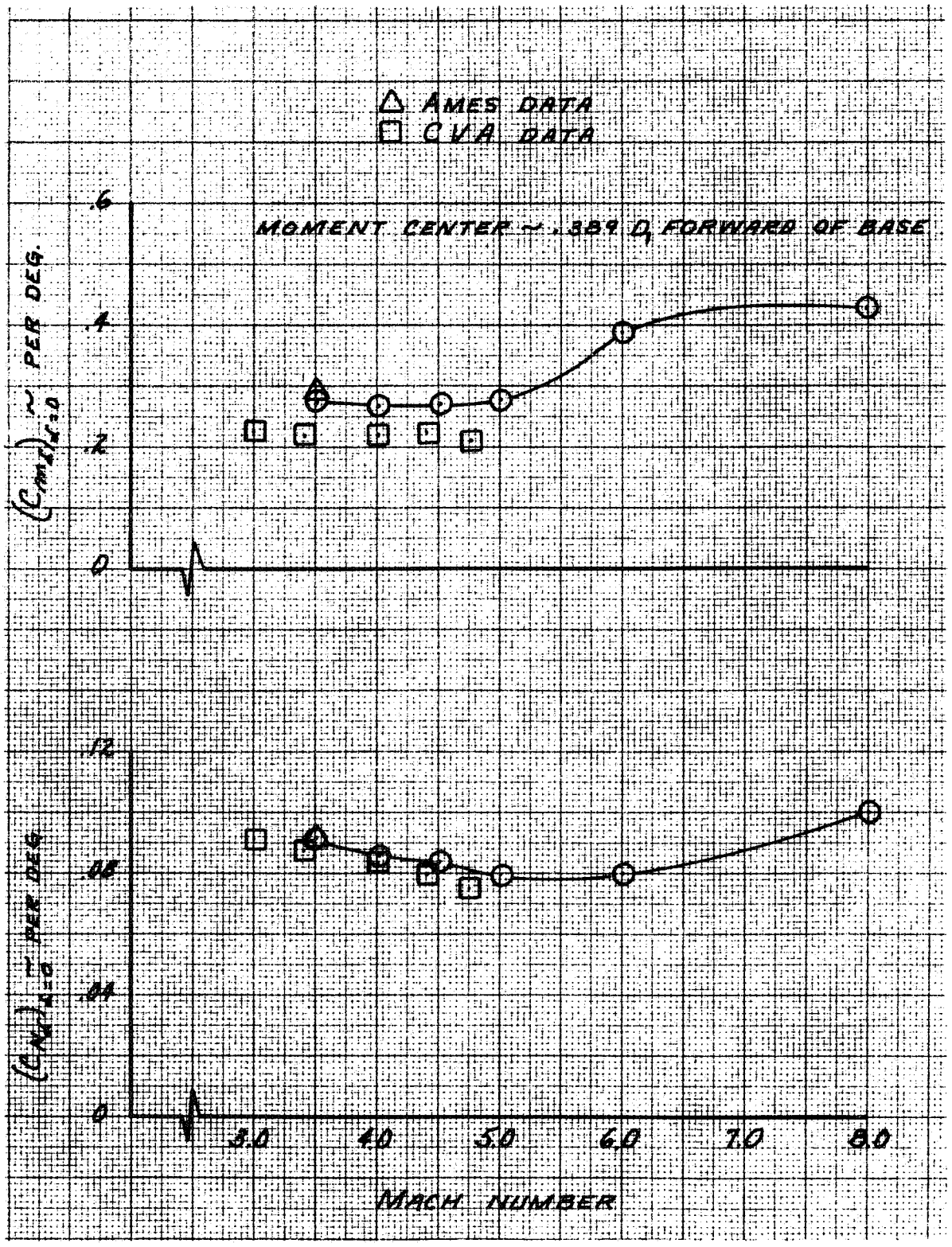

Figure 8. Effect of Mach Number on the Aerodynamic Coefficients for the Launch Configuration (Sheet 1 of 3)

CONFIDENTIAL

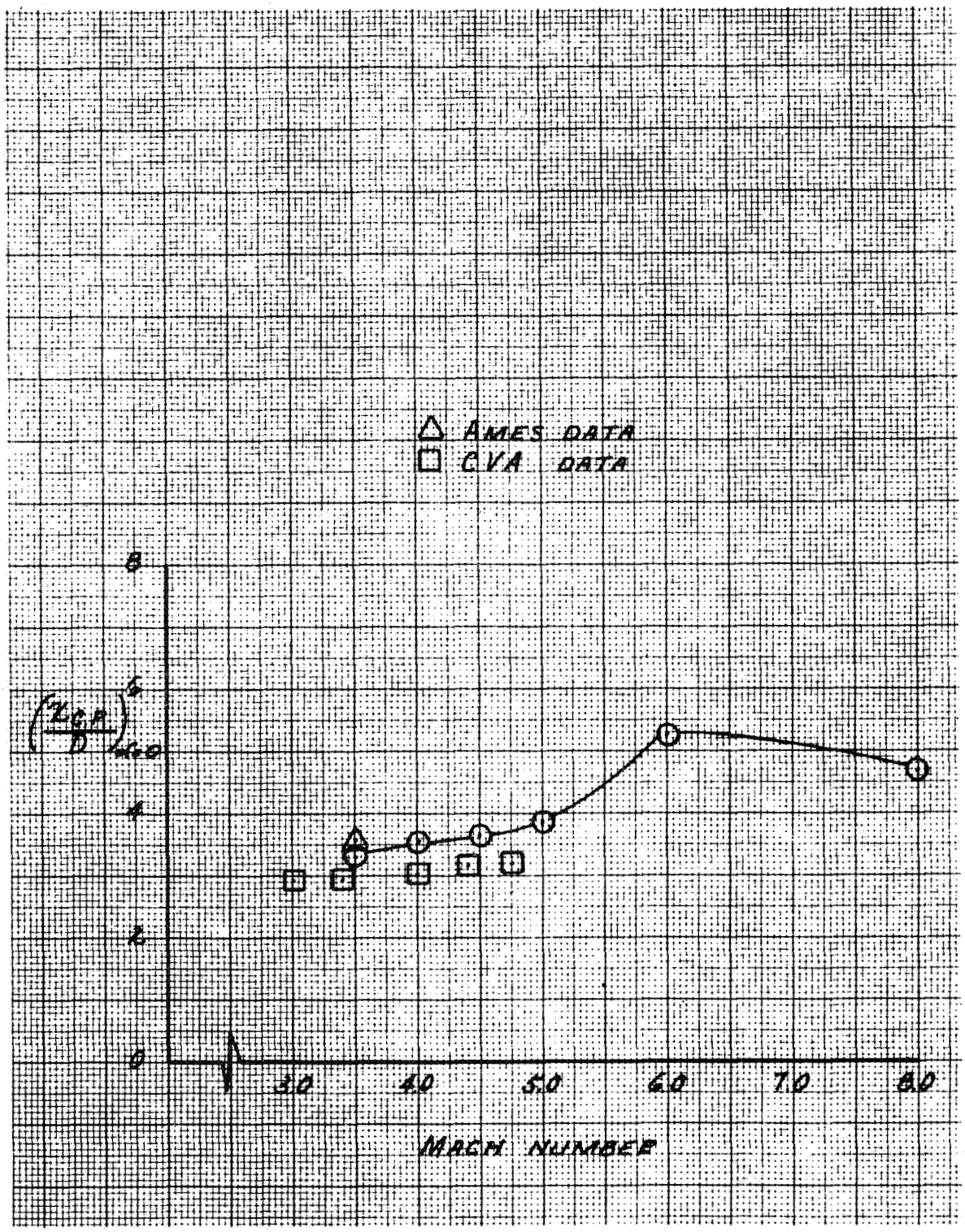

Figure 8. Effect of Mach Number on the Aerodynamic Coefficients for the Launch Configuration (Sheet 2 of 3)

CONFIDENTIAL

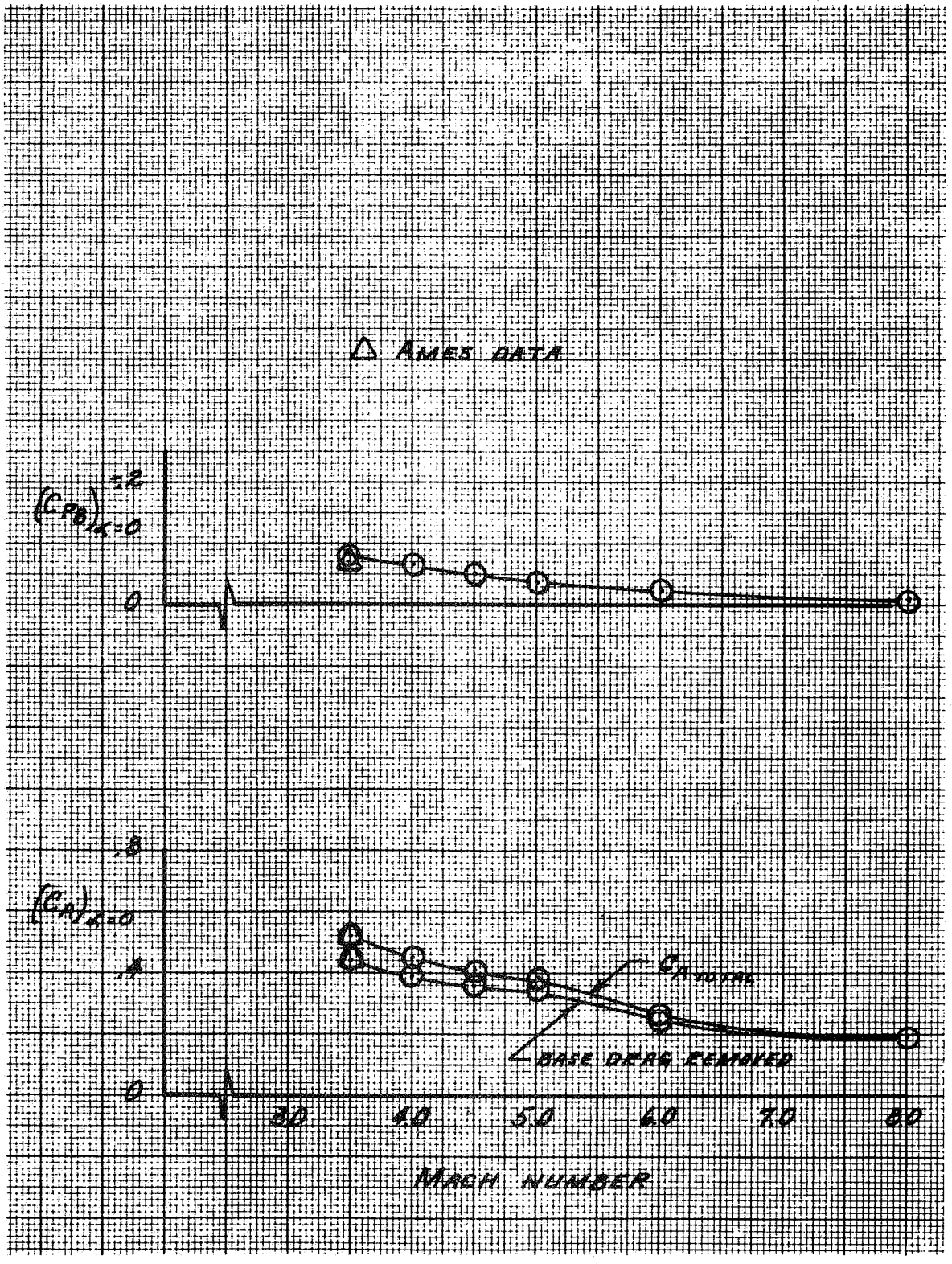

Figure 8. Effect of Mach Number on the Aerodynamic Coefficients for the Launch Configuration (Sheet 3 of 3)

CONFIDENTIAL

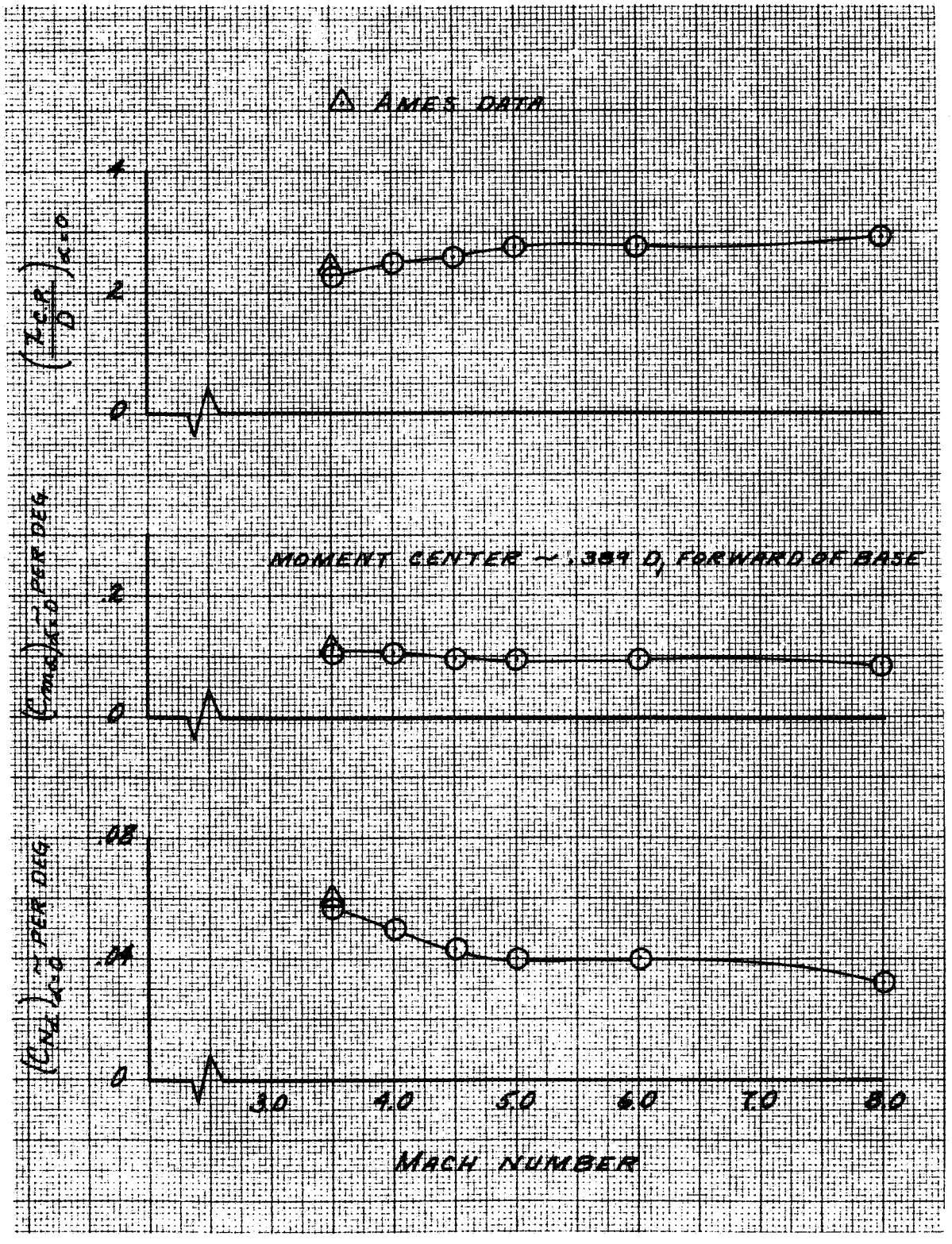

Figure 9. Effect of Mach Number on the Aerodynamic Coefficients for the Launch-Abort Configuration (sheet 1 of 2)

CONFIDENTIAL

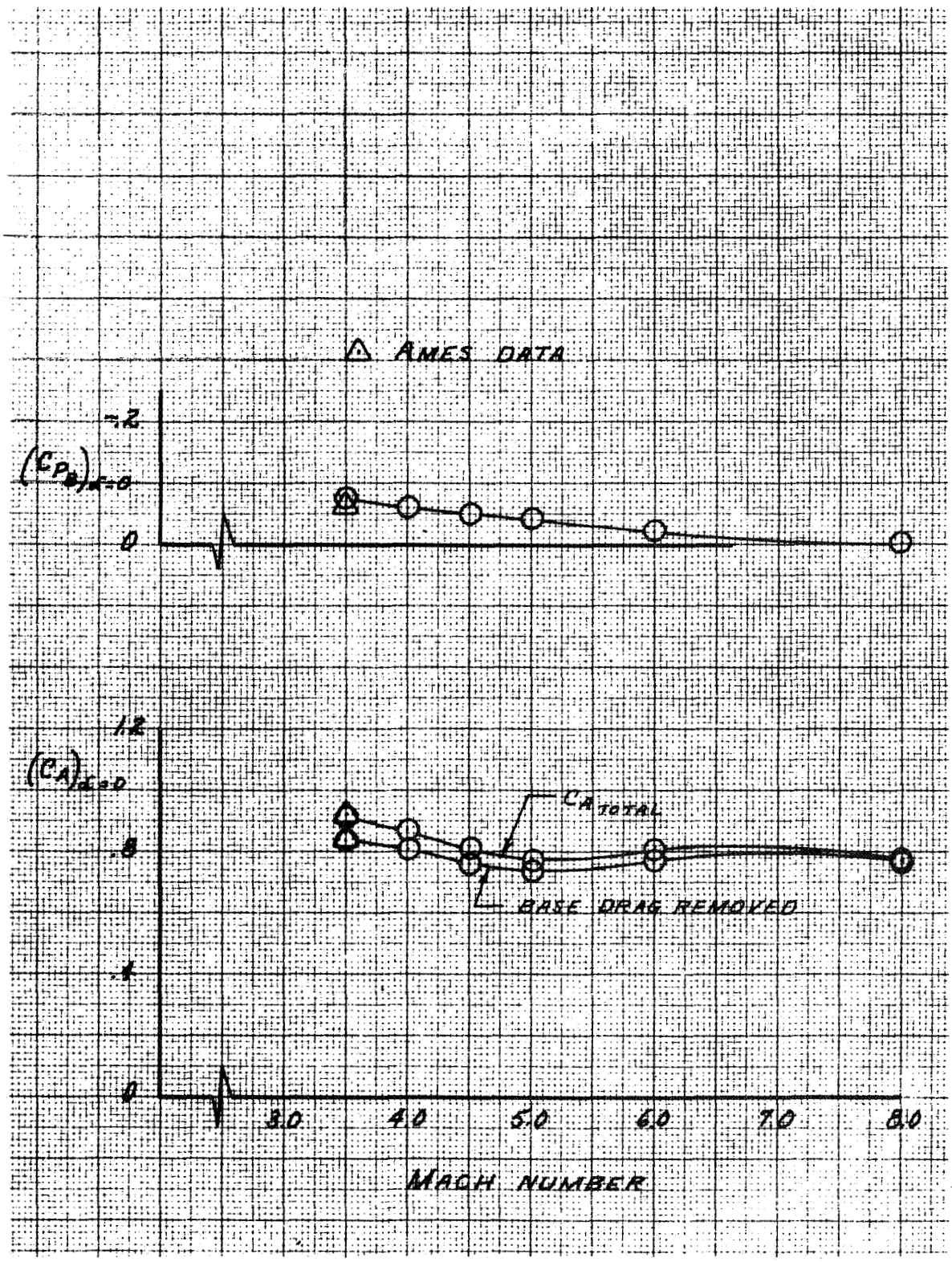

Figure 9. Effect of Mach Number on the Aerodynamic Coefficients for the Launch-Abort Configuration (sheet 2 of 2)

CONFIDENTIAL

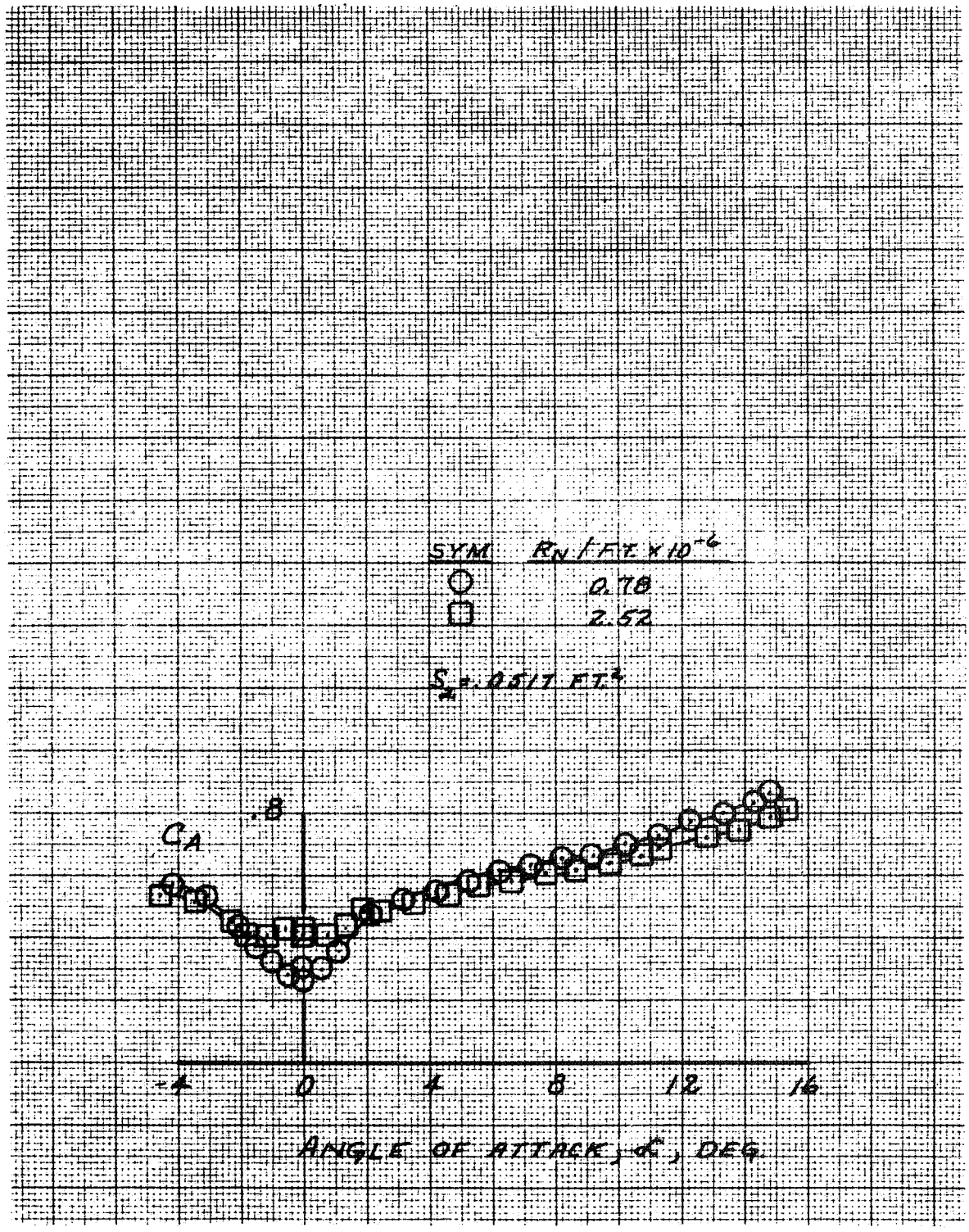

Figure 10. Effect of Reynolds Number on Axial Force Coefficient at Mach Number 8.0 for Second-Stage Configuration With Escape System

CONFIDENTIAL

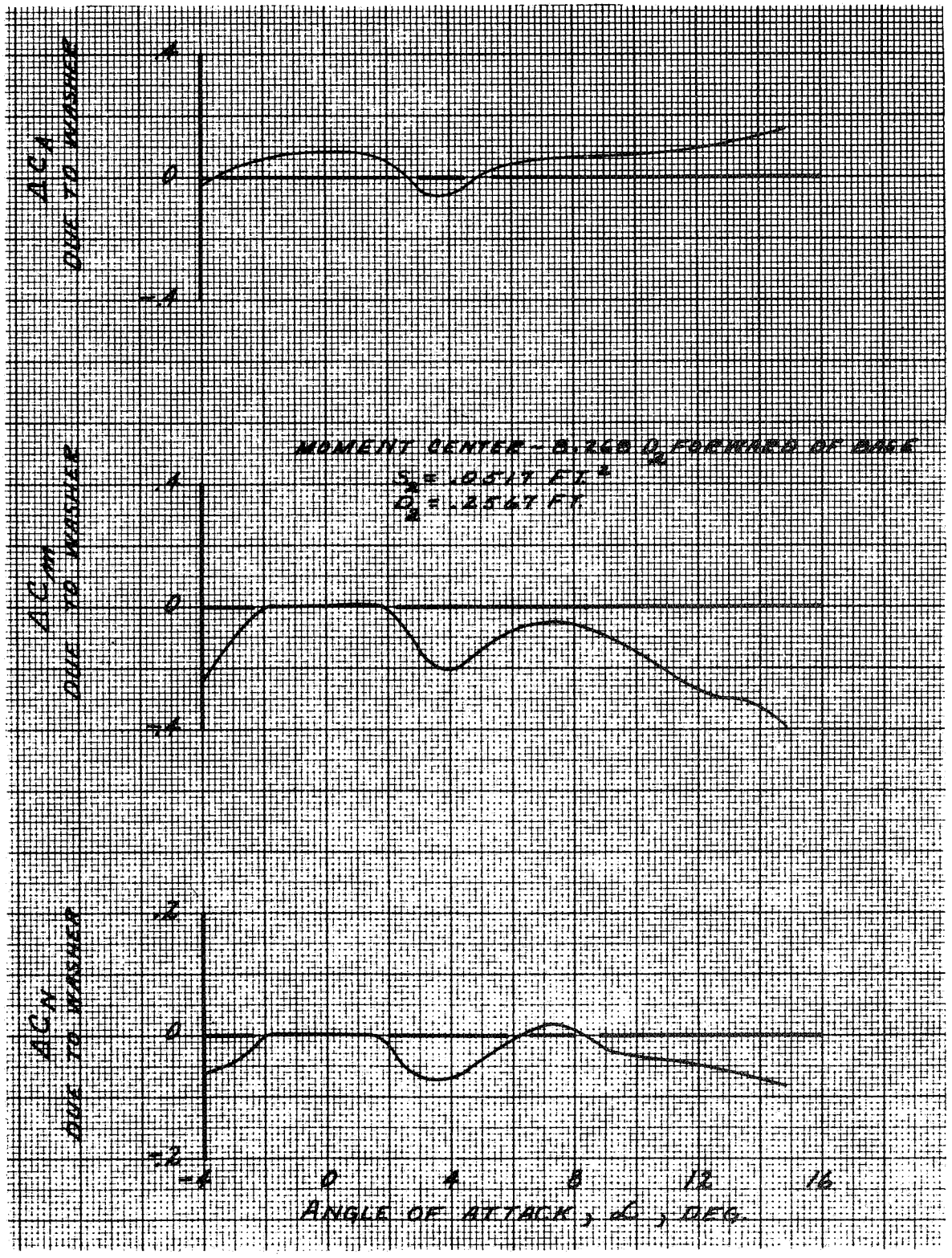

Figure 11. Effect of Launch Escape System Separator on Second-Stage Aerodynamic Characteristics at Mach Number 8.0

CONFIDENTIAL

CONFIDENTIAL

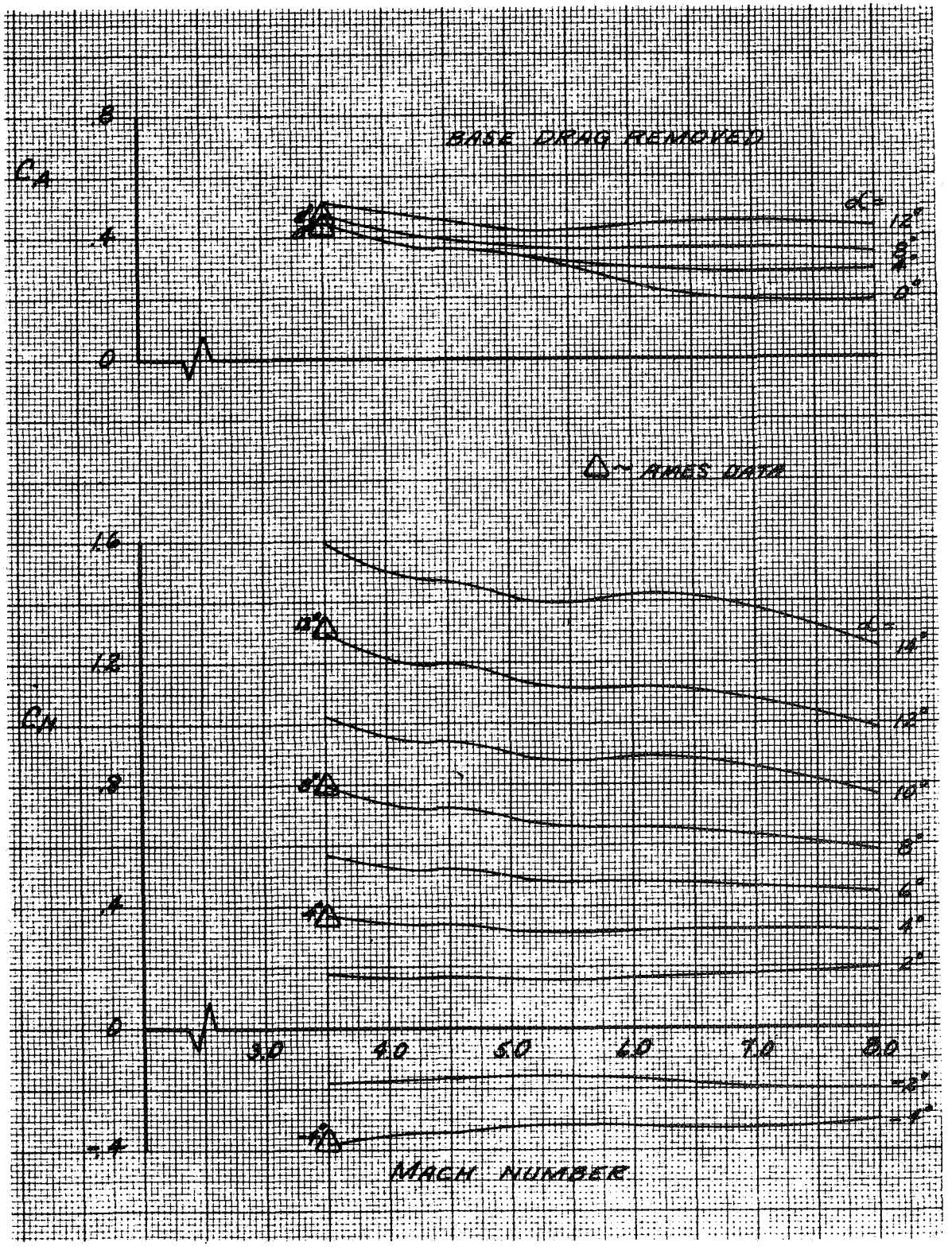

Figure 12. Effect of Mach Number on Aerodynamic Coefficients at Angles of Attack for the Launch Configuration (sheet 1 of 2)

CONFIDENTIAL

CONFIDENTIAL

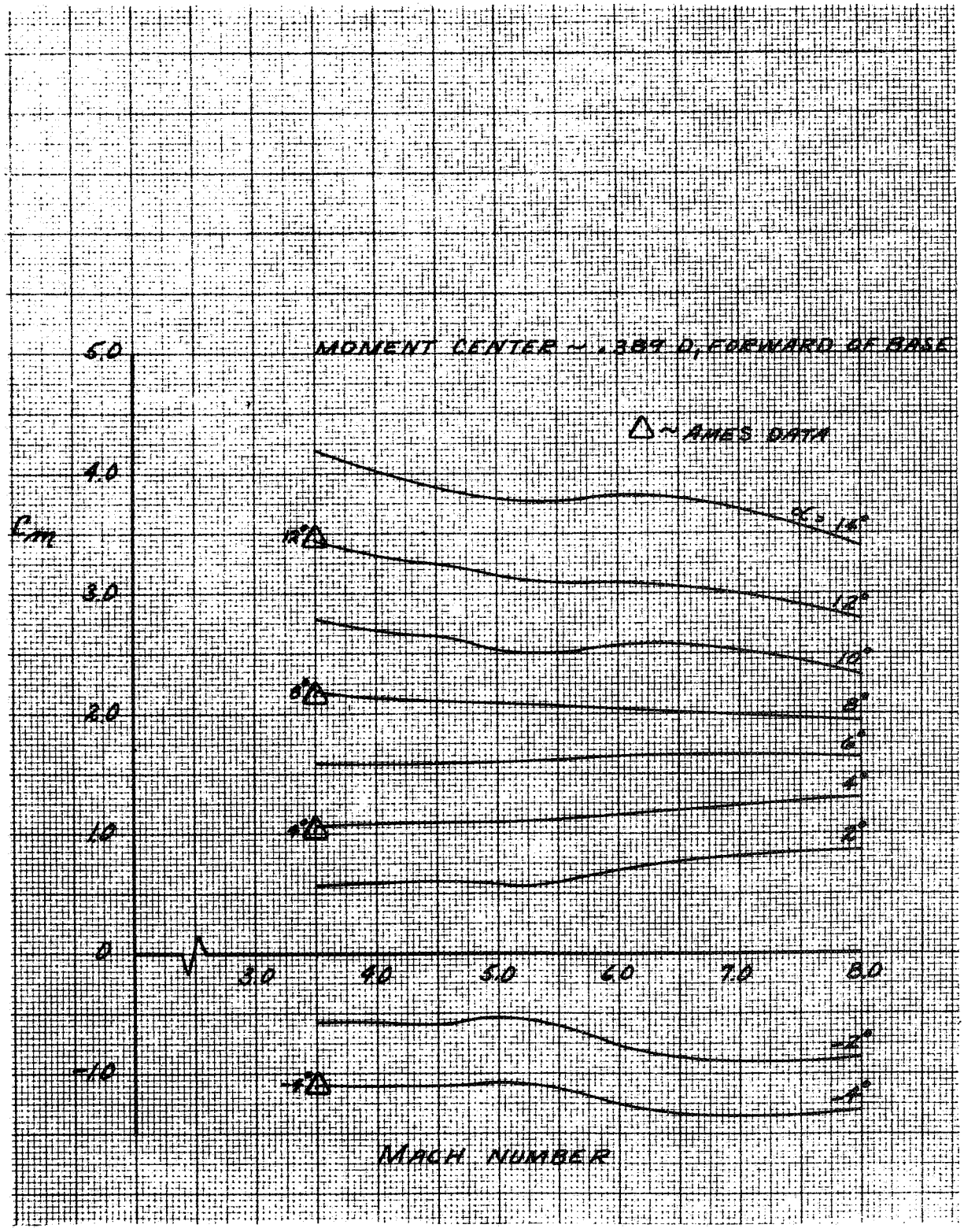

Figure 12. Effect of Mach Number on Aerodynamic Coefficients at Angles of Attack for the Launch Configuration (sheet 2 of 2)

CONFIDENTIAL

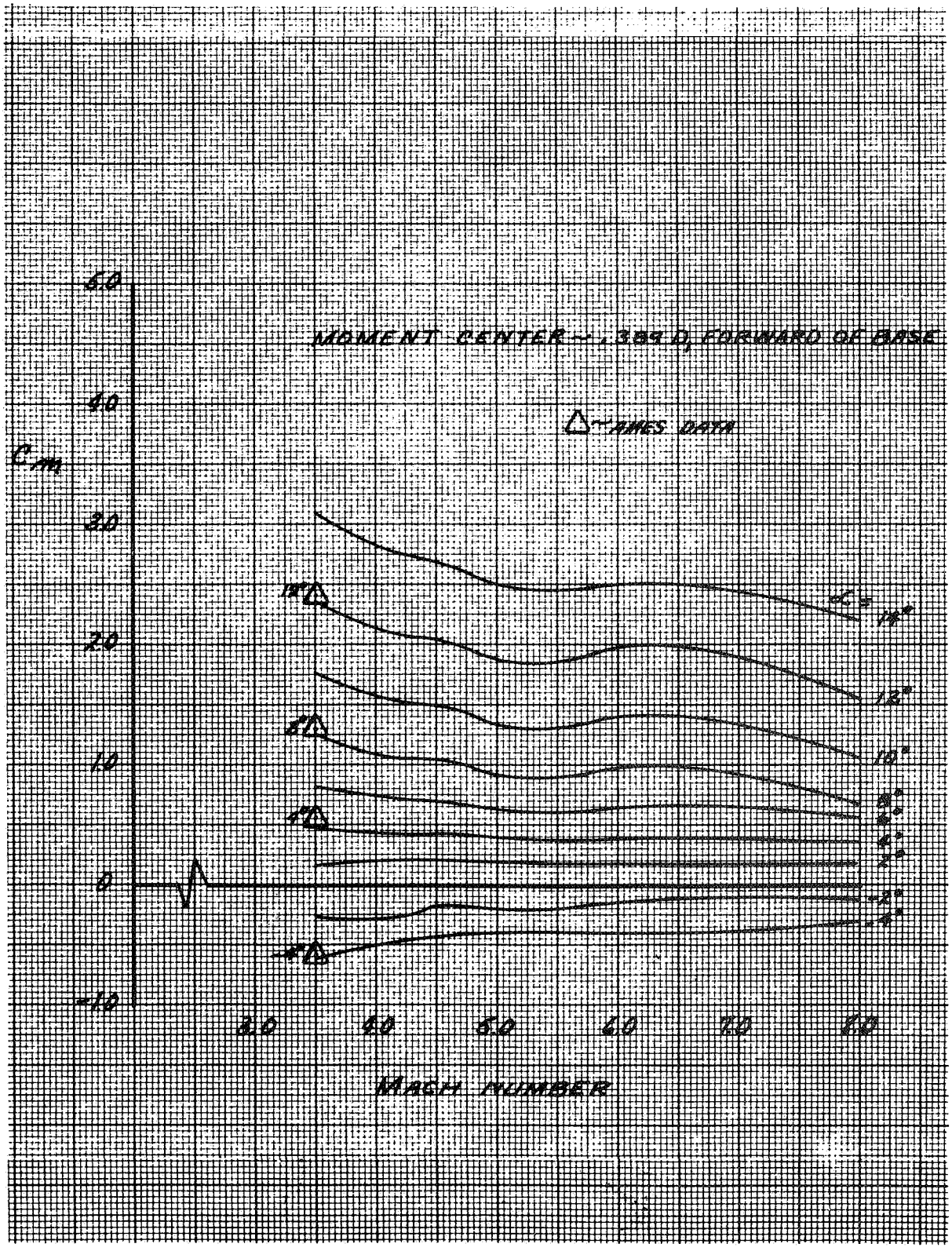

Figure 13. Effect of Mach Number on Aerodynamic Coefficients at Angles of Attack for the Launch-Abort Configuration (sheet 1 of 2)

CONFIDENTIAL

CONFIDENTIAL

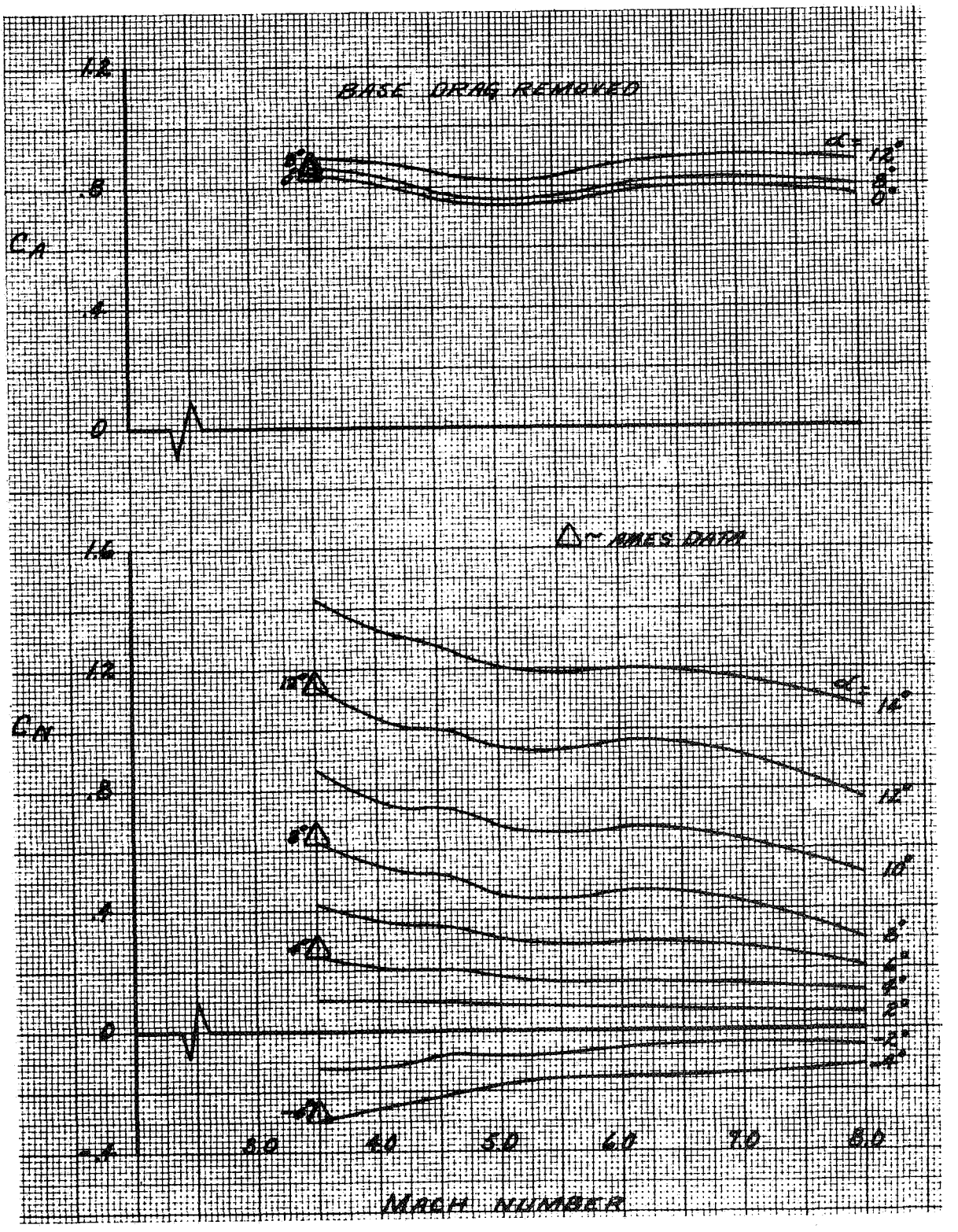

Figure 13. Effect of Mach Number on Aerodynamic Coefficients at Angles of Attack for the Launch-Abort Configuration (sheet 2 of 2)

CONFIDENTIAL

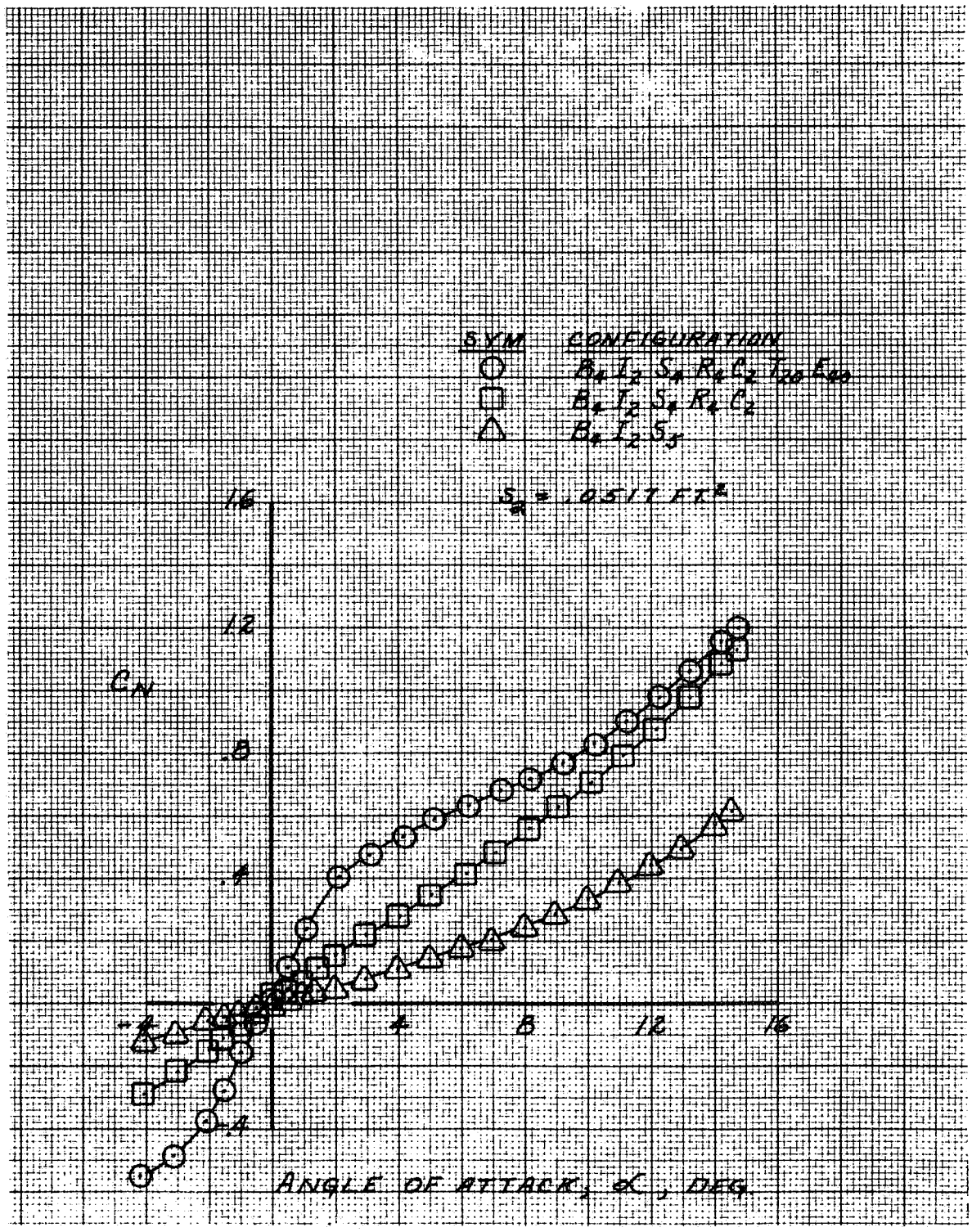

Figure 14. Effect of Angle of Attack on the Aerodynamic Coefficients at Mach Number 8.0 for the Second-Stage Configuration (sheet 1 of 3)

CONFIDENTIAL

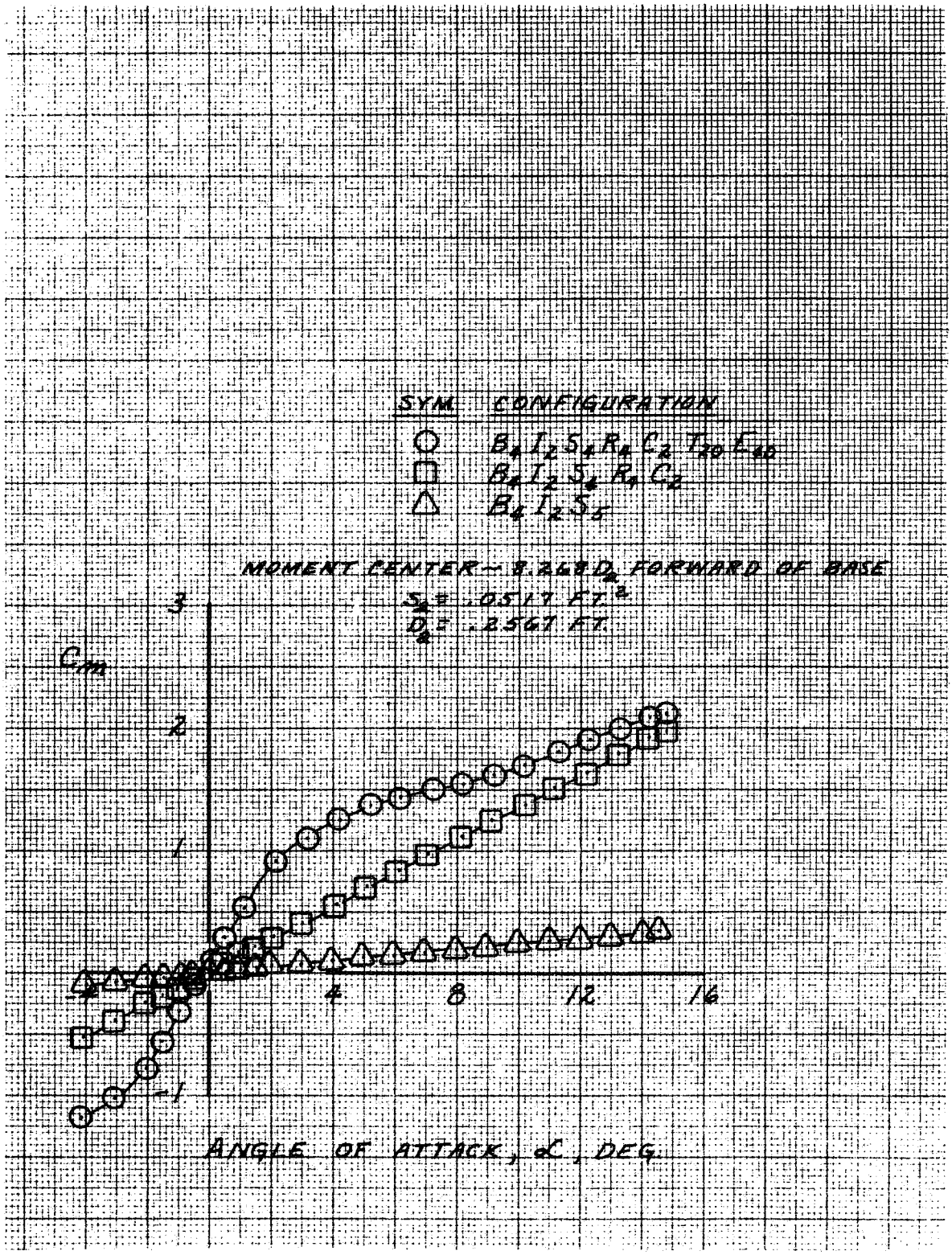

Figure 14. Effect of Angle of Attack on the Aerodynamic Coefficients at Mach Number 8.0 for the Second-Stage Configuration (sheet 2 of 3)

CONFIDENTIAL

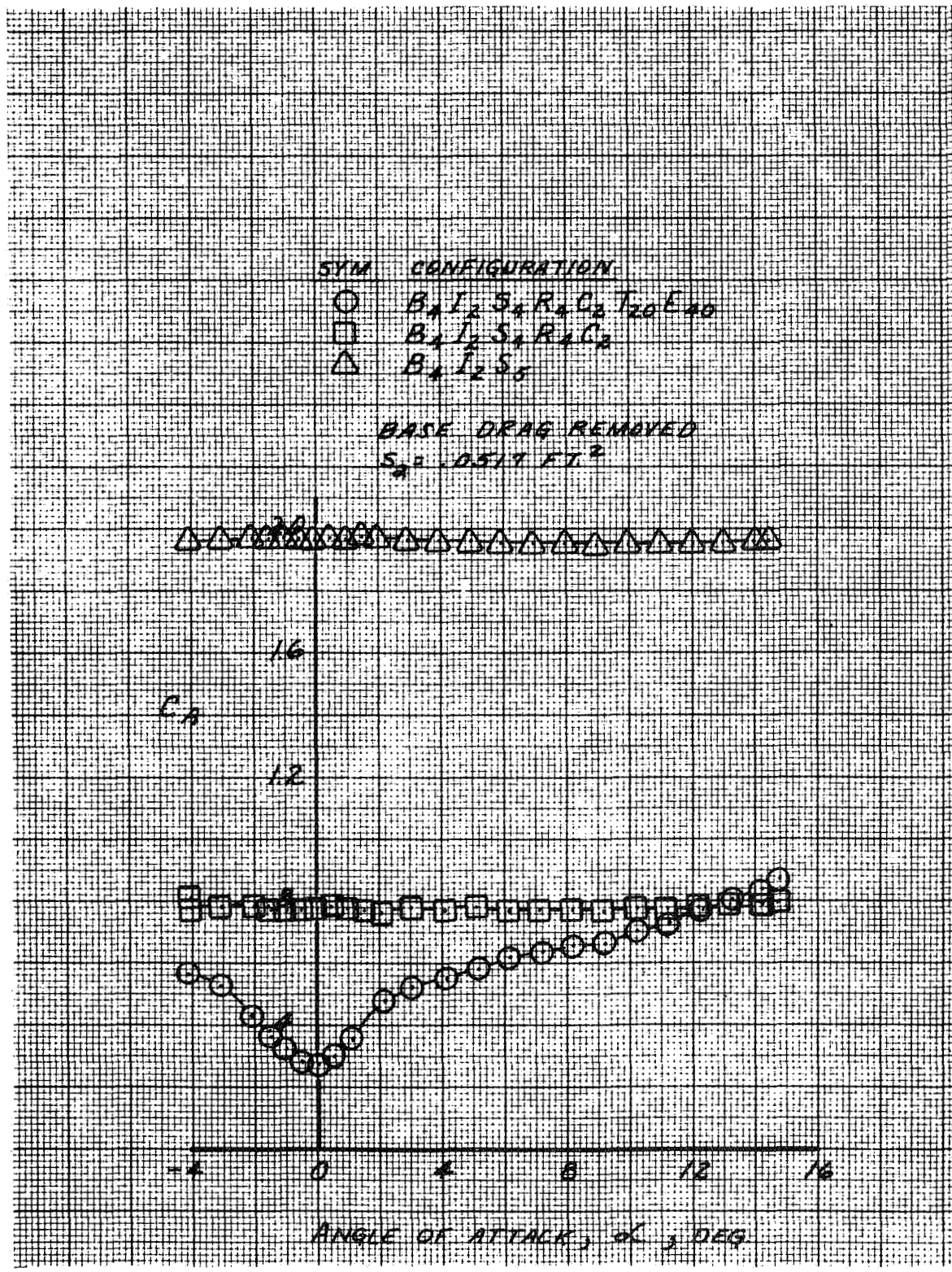

Figure 14. Effect of Angle of Attack on the Aerodynamic Coefficients at Mach Number 8.0 for the Second-Stage Configuration (sheet 3 of 3)

CONFIDENTIAL

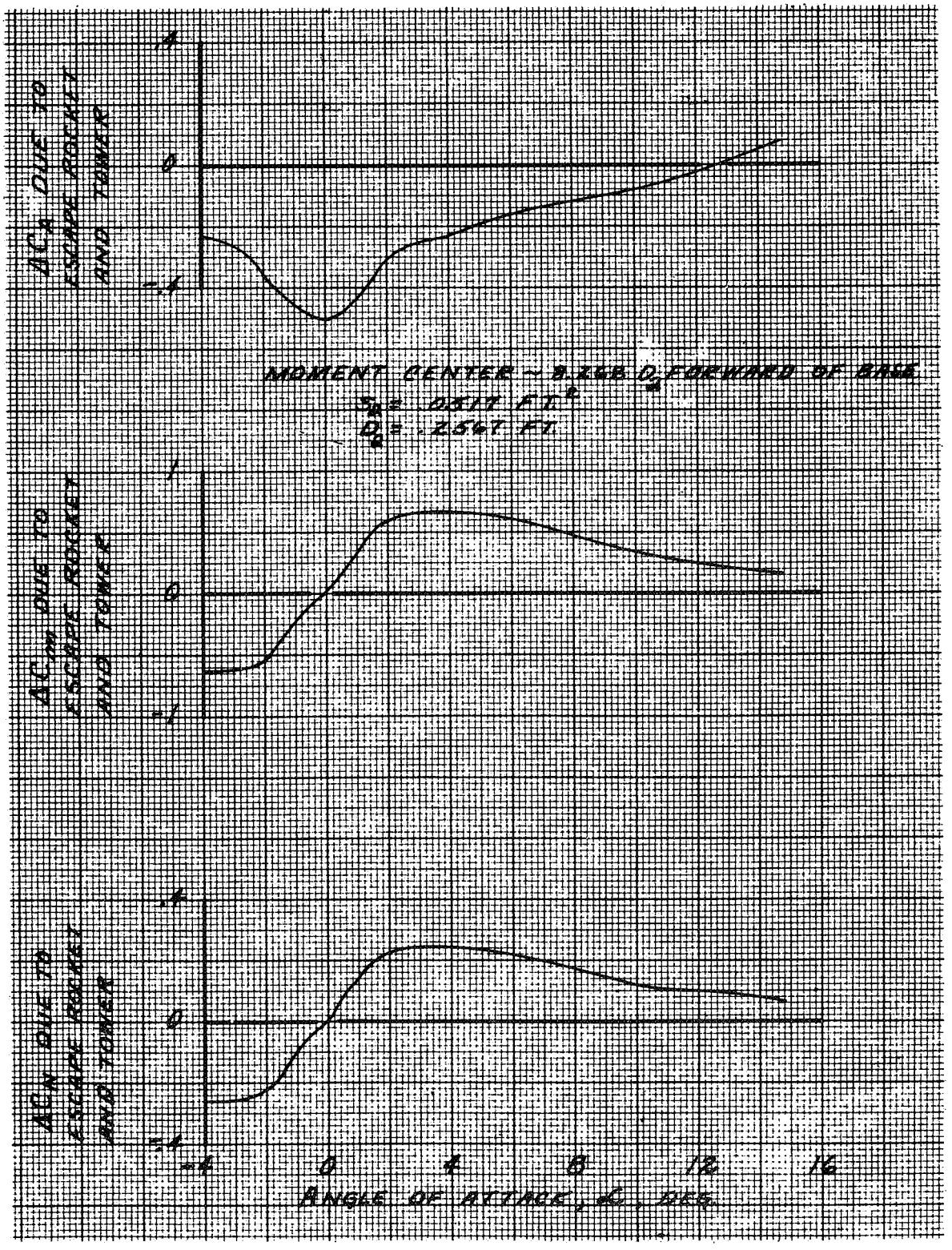

Figure 15. Effect of Escape Rocket and Tower (Separator On) on Second-Stage Aerodynamic Characteristics at Mach Number 8.0

IV. CONCLUSIONS

The static stability and force characteristics of the launch, launch-abort, and second-stage configurations of a 0.02-scale model of the Saturn C-1 launch vehicle with Apollo payload have been obtained in the Mach number range 3.50 to 8.0. The results of this investigation indicate the following conclusions.

1. At flight Reynolds numbers, the launch configuration force characteristics are significantly affected by flow separation at Mach number 6 and above.

2. The escape rocket and tower have a large effect on the force characteristics of the second-stage configuration at Mach number 8.0.

3. The Reynolds number variation at Mach number 8.0 resulted in a small change in axial force coefficient for the second-stage configuration. No significant effects attributable to Reynolds number variation were observed for the launch configuration at Mach number 6.0.

4. Removal of the flow separator had no measurable effect on the launch configuration aerodynamic characteristics. A small nonlinear effect due to the separator was observed for the second-stage configuration.

5. The aerodynamic coefficients were essentially insensitive to roll attitude.

CONFIDENTIAL

V. SYMBOLS

A_b	Model base area (used for computing base axial force), ft^2
C_A	Axial force coefficient with base axial force removed, $(C_{A_{total}} - C_{A_B})$
$C_{A_{total}}$	Axial force coefficient (including base effects), axial force/qS
C_{A_B}	Base axial force coefficient, $- C_{P_B} A_b/S$
C_ℓ	Rolling moment coefficient, rolling moment/qSD
C_m	Pitching moment coefficient about reference moment center, pitching moment/qSD
$\overline{C}_m$	Composite pitching moment coefficient, $\overline{C}_m = \sqrt{C_m^2 + C_n^2}$
C_{m_α}	Slope of pitching moment coefficient versus angle of attack, 1/deg
C_n	Yawing moment coefficient about reference moment center, yawing moment/qSD
C_N	Normal force coefficient, normal force/qS
$\overline{C}_N$	Composite normal force coefficient, $\overline{C}_N = \sqrt{C_N^2 + C_Y^2}$
C_{N_α}	Slope of normal force coefficient versus angle of attack, 1/deg
C_{P_B}	Base pressure coefficient, $(P_b - P_\infty)/q$
C_Y	Side force coefficient, side force/qS
D	Reference length, ft
M	Free-stream Mach number
P_b	Model base pressure, lb/ft^2
P_T	Free-stream stagnation pressure, lb/ft^2

P_∞	Free-stream static pressure, lb/ft^2
q	Free-stream dynamic pressure, lb/ft^2
R_N	Free-stream Reynolds number per ft
S	Reference area, ft^2
X_{cp}/D	Center of pressure location measured in reference lengths from the base, positive forward, $X_{cp}/D = \frac{C_m}{C_N} + \frac{\overline{X}}{D}$
$\overline{X}$	Location of reference moment center measured from the model base, ft
α	Angle of attack, deg
$\overline{\alpha}$	Composite angle of attack, $\cos \overline{\alpha} = \cos \alpha \cos \beta$
β	Angle of sideslip, deg
ϕ	Angle of roll, deg

The subscript $\alpha = 0$ denotes conditions existing at 0 angle of attack.

The base of the model is located at model station 0.000.